

Learning to Optimize in Model Predictive Control

Jacob Sacks* and Byron Boots*

Abstract—Sampling-based Model Predictive Control (MPC) is a flexible control framework that can reason about non-smooth dynamics and cost functions. Recently, significant work has focused on the use of machine learning to improve the performance of MPC, often through learning or fine-tuning the dynamics or cost function. In contrast, we focus on learning to *optimize* more effectively. In other words, to improve the update rule within MPC. We show that this can be particularly useful in sampling-based MPC, where we often wish to minimize the number of samples for computational reasons. Unfortunately, the cost of computational efficiency is a reduction in performance; fewer samples results in noisier updates. We show that we can contend with this noise by learning how to update the control distribution more effectively and make better use of the few samples that we have. Our learned controllers are trained via imitation learning to mimic an expert which has access to substantially more samples. We test the efficacy of our approach on multiple simulated robotics tasks in sample-constrained regimes and demonstrate that our approach can outperform a MPC controller with the same number of samples.

I. INTRODUCTION

Model Predictive Control (MPC) is a powerful, practical tool for solving sequential decision problems on real-world systems. MPC has been successfully used in a variety of tasks including autonomous helicopter aerobatics [1], aggressive off-road driving [2]–[4], manipulation [5], [6], and humanoid robot locomotion [7]. Recent work [4] has shown that many popular MPC algorithms can be unified through the generic framework of dynamic mirror descent (DMD) [8], a first-order online learning algorithm. This perspective provides an opportunity to improve performance of existing algorithms by drawing on powerful optimization techniques. Most modern approaches to optimization use fixed update rules tailored to specific classes of problems. Recently, research has explored *learning* to optimize [9], where the update rule is specified by a function approximator, such as a neural network, that can improve optimization performance with experience.

In this work, we leverage the optimization perspective of sampling-based MPC and adopt the learning-to-optimize framework in order to improve the update rule. This is in contrast to most existing learning-based approaches to MPC, which either focus on learning a good dynamics model [3], [10]–[15], introducing a learned cost-shaping term into the objective [16], coupling MPC with a learned value function [17]–[20], or learning a good warm-start for MPC to refine [21]. Other approaches have focused on performing MPC with a learned latent space of high-dimensional observations [15], [22]–[27], low-level skills [28], or controls such that sampling because more efficient

[29]. Another promising avenue has explored differentiating through optimal controllers or planners to learn components of the optimization pipeline. These methods propose to learn or fine-tune the dynamics and cost functions of the controllers [16], [29]–[34] or parameters of differentiable planners [35]–[38] end-to-end. Compared with these approaches, we fix the dynamics and cost function and instead focus on improving the optimization process.

For many practical sampling-based MPC algorithms, the primary challenge is finding a good trade-off between speed and accuracy. Sampling-based MPC algorithms work by using simple policies to sample control sequences, which are used to roll out the dynamics function and compute a sample-based approximation of the gradient of the objective function. This approximate gradient is then used to update the sampling policy. Using complex dynamics and cost functions can make each rollout computationally expensive. To contend with this problem, one could use fewer samples to decrease computation, but this can increase the noise in the sample-based gradient, leading to poor performance.

In this paper, our objective is to *learn* how to more effectively update the control distribution with a small number of samples. To this end, we employ imitation learning to train fast, low-sample controllers to imitate an expert which makes use of additional samples. The learned optimizer is better able to integrate information in the sample-constrained regime. Our key contributions are that we:

- 1) Leverage the gradient-based interpretation of many sampling-based MPC algorithms and show how to improve performance by learning a better update rule.
- 2) Propose to use structured sampling techniques to provide more information to the learned update than is contained in the noisy gradient, which enables us to make better use of fewer samples.
- 3) Empirically evaluate our proposed approach on multiple simulated robotics tasks, in which the learned optimizer has restricted access to samples.

Our experiments show that the learned controller is indeed able to make better use of fewer samples while remaining competitive or outperforming the expert with the same number of samples. This illustrates the utility of the learning-to-optimize framework in the domain of control and indicates the potential to improve the viability of sampling-based MPC controllers on embedded platforms.

II. BACKGROUND

A. Model Predictive Control

We consider the problem of controlling a discrete-time stochastic dynamical system with states $x_t \in \mathbb{R}^N$ and controls

*University of Washington, Seattle WA 98105, USA. {jsacks6, bboots}@cs.washington.edu

$u_t \in \mathbb{R}^M$. The system chooses controls using a policy π_{θ_t} with parameters $\theta_t \in \Theta$, where Θ is the set of feasible parameters. After applying the control, the system incurs the instantaneous cost $c(x_t, u_t)$ and transitions to the next state x_{t+1} according to the dynamics

$$x_{t+1} \sim f(x_t, u_t), \quad (1)$$

where $f: \mathbb{R}^N \times \mathbb{R}^M \rightarrow \mathbb{R}^N$ is a stochastic transition map. Over a time horizon H , we sample a control sequence $U_t \triangleq (u_t, u_{t+1}, \dots, u_{t+H-1})$, which results in a state trajectory $X_t \triangleq (x_t, x_{t+1}, \dots, x_{t+H})$. The total cost incurred is

$$C(X_t, U_t) = \sum_{h=0}^{H-1} c(x_{t+h}, u_{t+h}) + c_{term}(x_{t+H}), \quad (2)$$

where $c_{term}(\cdot)$ is a terminal cost function. The goal of MPC is to find the optimal set of parameters $\theta_t \triangleq (\theta_t, \theta_{t+1}, \dots, \theta_{t+H-1})$ for the sequence of policies $\pi_{\theta_t} \triangleq (\pi_{\theta_t}, \pi_{\theta_{t+1}}, \dots, \pi_{\theta_{t+H-1}})$. At each time step, we solve

$$\theta_t \leftarrow \arg \min_{\theta \in \Theta} J(\pi_{\theta}; x_t), \quad (3)$$

where $J(\cdot)$ is a statistic defined on cost $C(X_t, U_t)$ such that its minimum occurs at the optimal θ_t . In general, we do not have access to the true dynamics function f and instead approximate it with the model \hat{f} , corresponding to the surrogate statistic $\hat{J}(\pi_{\theta}; x_t)$.

This optimization problem can only be approximated in practice due to real-time constraints. One commonly applied heuristic is to bootstrap the previous approximate solution as an initialization for the current problem. This is effective because the optimization problems between two consecutive time steps share all control variables except the first and last. If our solution from the previous problem is θ_{t-1} , then our warm start for the current problem is given by

$$\tilde{\theta}_t = \Phi(\theta_{t-1}), \quad (4)$$

where $\Phi(\cdot)$ is called the shift operator [4]. A common choice is $\tilde{\theta}_t = (\theta_{t+1}, \theta_{t+2}, \dots, \theta_{t+H-1}, \bar{\theta})$, where $\bar{\theta}$ is a new parameter which reflects the expected final action.

Recent work by Wagener et al. [4] showed that many common MPC algorithms fall under the framework of an online learning algorithm known as dynamic mirror descent (DMD) [8]. Online learning involves interactions between a learner and an environment over T rounds. In our case, the learner is the MPC algorithm, which in round t plays the decision $\tilde{\theta}_t \in \Theta$, the shifted policy parameter sequence, along with side information u_{t-1} , the control applied to the real system. The per-round loss is defined as $\ell_t(\cdot) = \hat{J}(\cdot; x_t)$, which is selected by the environment via the state transition. At round t , DMD updates the parameters by the rule:

$$\theta_t \leftarrow \arg \min_{\theta \in \Theta} (\gamma_t g_t, \theta) + D_{\psi}(\theta || \tilde{\theta}_t), \quad (5)$$

where $g_t = \nabla \ell_t(\tilde{\theta}_t)$, $\gamma_t > 0$ is the step size, and $D_{\psi}(\theta || \theta') = \psi(\theta) - \psi(\theta') - \langle \nabla \psi(\theta'), \theta - \theta' \rangle$ is the Bregman divergence generated by a strictly convex function ψ on θ . Solving MPC with DMD is known as *DMD-MPC* and includes a family of common MPC algorithms as special cases [4].

B. Sampling-Based Model Predictive Control

A popular, practical sampling-based MPC algorithm is Model Predictive Path Integral (MPPI) control [2], [3], which is a special case of DMD-MPC under certain choices of objective function, control distribution, and Bregman divergence [4]. Specifically, we assume the policies are open loop and choose the exponential utility for the objective:

$$\ell_t(\theta) = -\log \mathbb{E}_{\pi_{\theta, \hat{f}}} \left[\exp \left(-\frac{1}{\lambda} C(X_t, U_t) \right) \right], \quad (6)$$

where $\lambda > 0$ is a scaling parameter, also known as the temperature. Since we generally assume that the cost function is non-differentiable with respect to θ , we instead compute the gradients via a likelihood-ratio derivative:

$$\nabla \ell_t(\theta) = -\frac{\mathbb{E}_{\pi_{\theta, \hat{f}}} \left[\exp \left(-\frac{1}{\lambda} C(X_t, U_t) \right) \nabla_{\theta} \log \pi_{\theta}(U_t) \right]}{\mathbb{E}_{\pi_{\theta, \hat{f}}} \left[\exp \left(-\frac{1}{\lambda} C(X_t, U_t) \right) \right]}, \quad (7)$$

We approximate these expectations with Monte Carlo sampling, which results in a convex combination of gradients:

$$\nabla \ell_t(\theta) = -\sum_{i=1}^N w_i \nabla_{\theta} \log \pi_{\theta}(U_t), \quad (8)$$

with weights w_i defined by the softmax operation

$$w_i = \frac{e^{-\frac{1}{\lambda} C(X_t^{(i)}, U_t^{(i)})}}{\sum_{j=1}^N e^{-\frac{1}{\lambda} C(X_t^{(j)}, U_t^{(j)})}}. \quad (9)$$

Because of this estimation, the gradients will be noisy, with noise that scales inversely with number of samples. The more samples we use, the more exact our approximations will be.

Next, we choose the Bregman divergence to be the KL divergence and the distribution to be a factorized Gaussian:

$$\pi_{\theta}(U_t) = \prod_{h=0}^{H-1} \pi_{\theta_h}(u_{t+h}) = \prod_{h=0}^{H-1} \mathcal{N}(u_{t+h}; \mu_{t+h}, \Sigma_{t+h}), \quad (10)$$

for some mean vectors μ_{t+h} and covariance matrices Σ_{t+h} . Under these assumptions, Wagener et al. [4] showed that the solution to Equation (5) becomes

$$\begin{aligned} \mu_{t+h} &= (1 - \gamma_t^{\mu}) \tilde{\mu}_{t+h} + \gamma_t^{\mu} \frac{\mathbb{E}_{\pi_{\theta, \hat{f}}} \left[e^{-\frac{1}{\lambda} C(X_t, U_t)} u_{t+h} \right]}{\mathbb{E}_{\pi_{\theta, \hat{f}}} \left[e^{-\frac{1}{\lambda} C(X_t, U_t)} \right]}, \\ \Sigma_{t+h} &= (1 - \gamma_t^{\sigma}) \tilde{\Sigma}_{t+h} + \gamma_t^{\sigma} \frac{\mathbb{E}_{\pi_{\theta, \hat{f}}} \left[e^{-\frac{1}{\lambda} C(X_t, U_t)} m_{t+h} m_{t+h}^T \right]}{\mathbb{E}_{\pi_{\theta, \hat{f}}} \left[e^{-\frac{1}{\lambda} C(X_t, U_t)} \right]}, \end{aligned} \quad (11)$$

where $m_{t+h} = u_{t+h} - \mu_{t+h}$ and γ_t^{μ} and γ_t^{σ} are step sizes for the mean and covariance, respectively. When we use the Monte-Carlo approximations to the gradients in Equation (8), this results in the following update:

$$\begin{aligned} \mu_{t+h} &= (1 - \gamma_t^{\mu}) \tilde{\mu}_{t+h} + \gamma_t^{\mu} \sum_{i=1}^N w_i u_{t+h}^{(i)} \\ \Sigma_{t+h} &= (1 - \gamma_t^{\sigma}) \tilde{\Sigma}_{t+h} + \gamma_t^{\sigma} \sum_{i=1}^N w_i m_{t+h}^{(i)} m_{t+h}^{(i)T}, \end{aligned} \quad (12)$$

This update equation is the same as the MPPI update rule when $\gamma_t^{\mu} = 1$ and we do not update the covariance.

C. Learning to Optimize Framework

Rather than hand design an update rule tailored to a specific subclass of problems, the learning-to-optimize approach aims to learn a sequential update rule from experience. For a set of optimizee parameters $\theta \in \Theta$ and objective function $\ell(\theta)$, we find the minimizer $\theta^* = \arg \min_{\theta \in \Theta} \ell(\theta)$ with an iterative algorithm that has the update rule

$$\theta_{t+1} = m_\phi(\theta_t, t), \quad (13)$$

where m is the learned optimizer, which can be of any parameterized function class with parameters ϕ .

The majority of approaches to learning-to-optimize differentiate through the optimization process using gradient descent [39]–[43] or use reinforcement learning [44]–[47]. However, we do not assume that the optimization process is end-to-end differentiable and wish to avoid the high sample complexity that often hinders reinforcement learning. Instead, we opt to use imitation learning to train the optimizer. Chen et al. [43] also make use of imitation learning, in which the experts are common hand-designed optimizers that have access to full gradient information. However, in our case, the learned optimizers only have access to noisier gradients than the expert demonstrator and therefore less information.

Another major difference from prior work is that most literature in this area targets optimizing deep neural networks. As such, they must contend with the large parameter space of these models. Andrychowicz et al. [39] proposed to use a coordinate-wise optimizer, in which the parameters of the optimizer are shared across updates for all optimizee parameters. A downside to this approach is that it throws away potentially useful information for improving the learned update. Instead, since we have a moderate number of parameters, we can jointly optimize the entire planning horizon of control distribution parameters in order to capture relationships between time steps.

III. LEARNING TO OPTIMIZE FOR CONTROL

A. Design of the Learnable Optimizer

As shown in the previous section, the MPPI update rule in Equation (12) corresponds to performing mirror descent with an approximate gradient computed from N samples. Fewer samples results in a worse approximation and, therefore, a noisier update. One possible avenue for improving performance would be to employ more advanced first-order methods [48]–[53]. However, by adopting the learning-to-optimize framework and replacing the update rule with a learned optimizer, we can potentially do better than a manually specified update. A naive approach would be to follow Equation (13) and use the noisy gradient as input to the learned optimizer to produce the updated parameters. However, our objective is to learn how to mitigate the effect of a low number of samples on gradient noise, and the computation of the noisy gradient itself potentially throws away information that may be useful for improving the update. For instance, looking at Equation (12), we are simply computing a weighted sum of the samples. This collapses the information in each trajectory sample and its corresponding

cost into a single vector. Therefore, we propose instead to use the individual components which form the gradient directly.

From Equation (12), we can see that the update is a function of the current mean $\tilde{\mu}_{t+h}$ and covariance $\tilde{\Sigma}_{t+h}$, sample weights $w_t^{(1:N)}$, and control samples $u_{t+h}^{(1:N)}$. The sample weights themselves are actually a function of the total trajectory costs $C_t^{(1:N)}$, where $C_t = C(X_t, U_t)$. One potential choice would be to make each of these terms an input to the learned update:

$$\mu_{t+h}, \Sigma_{t+h} = m_\phi\left(\tilde{\mu}_{t+h}, \tilde{\Sigma}_{t+h}, C_t^{(1:N)}, u_{t+h}^{(1:N)}\right). \quad (14)$$

A limitation of this choice of parameterization is that it assumes independence of the updates between time steps in the rollouts. While this is the case for vanilla MPPI [2], [3], we could potentially learn a better update by incorporating information across time steps. However, if we parameterize the optimizer with a fully-connected or recurrent neural network architecture, this would result in a large number of parameters to learn, making optimization difficult. Instead, we alter the way in which we sample from the Gaussian policies to remedy this explosion in the dimensionality.

As proposed by Bhardwaj et al. [6], we make use of low-discrepancy Halton sequences [54] to generate samples from the Gaussian policies. Normal pseudo-random sequences often result in clusters of sampled points, leaving many regions of the parameter space untouched. Low-discrepancy sequences are a deterministic alternative that alleviate this problem by correlating each point. A D -dimensional Halton sequence x_1, x_2, \dots, x_N , in which $x_i \in \mathbb{R}^D$ is generated by

$$x_i = (\phi_{p_1}(i), \dots, \phi_{p_D}(i)), \quad \phi_{p_b}(i) = \sum_{j=1}^{\infty} a_j(p_b) p_b^{-j}, \quad (15)$$

where p_1, \dots, p_D are consecutive prime numbers and $a_j(p_b) \in \{0, 1, \dots, p_b - 1\}$ such that the condition $i = \sum_{j=1}^{\infty} a_j(p_b) p_b^{j-1}$ holds. The Halton sequence is sampled once at the beginning of the rollout and then transformed using the mean and covariance of the Gaussian policy. While this can improve the performance of sampling-based MPC, the main benefit is that it makes all sampled control sequences a deterministic function of the current mean and covariance. Therefore, the sampled control sequences can be excluded from the learned update without loss of information.

As such, rather than optimizing each time step independently, we leverage the structured nature of these samples to learn an update that optimizes the entire trajectory jointly using only cost information. The resulting update is then

$$\mu_t, \Sigma_t = m_\phi\left(\tilde{\mu}_t, \tilde{\Sigma}_t, C_t^{(1:N)}\right), \quad (16)$$

where $\mu_t \triangleq (\mu_t, \mu_{t+1}, \dots, \mu_{t+H-1})$, $\Sigma_t \triangleq (\Sigma_t, \Sigma_{t+1}, \dots, \Sigma_{t+H-1})$, and $\tilde{\mu}_t$ and $\tilde{\Sigma}_t$ are defined similarly. We can think about the Halton sequence as giving us a sense of what the environment and cost landscape is like around the current state. Since the learned optimizer can potentially make better use of its inputs than the expert, we may be able to more effectively use fewer samples while maintaining similar performance.

Algorithm 1: DAGGER Training Loop

Input: Initial bootstrapped dataset \mathcal{D} , initial policy $\pi_{\tilde{\theta}_1}$, initial state distribution ρ
Parameters: Iterations K , probabilities $\{\beta_k\}_{k=1}^K$, rollouts per iteration R

for $k = 1, 2, \dots, K$ **do**
 Initialize dataset $\mathcal{D}_i \leftarrow \emptyset$
 for $r = 1, 2, \dots, R$ **do**
 Sample initial state $x_1 \sim \rho$
 $\tilde{\theta}_{1:T}, C_{1:T}^{(1:M)}, \theta_{1:T}^{expert} \leftarrow \text{Rollout}(x_1, \pi_{\tilde{\theta}_1}, \beta_k)$
 Append $\mathcal{D}_i \leftarrow \mathcal{D}_i \cup \{(\tilde{\theta}_{1:T}, C_{1:T}^{(1:M)}, \theta_{1:T}^{expert})\}$
 end
 Aggregate datasets $\mathcal{D} \leftarrow \mathcal{D} \cup \mathcal{D}_i$
 Train optimizer parameters ϕ on \mathcal{D}
end

Finally, we note that Equation (12) is a convex combination of the previous control parameters and the weighted samples. We can actually think about MPC as a form of recurrent network, with the warm-started control distribution as our form of memory about the previous time steps. From this perspective, the step size is acting as a gating term which modulates how much information we preserve about our history. The hidden state update in a gated recurrent unit (GRU) [55] is of the same form, except the multiplicative gating term is also learned. Inspired by this similarity, we use the following update:

$$\begin{aligned} g_t^\mu, g_t^\sigma, h_t^\mu, h_t^\sigma &= m_\phi(\tilde{\mu}_t, \tilde{\Sigma}_t, C_t^{(1:N)}) \\ \mu_t &= (1 - g_t^\mu) \odot \tilde{\mu}_t + g_t^\mu \odot h_t^\mu \\ \Sigma_t &= (1 - g_t^\sigma) \odot \tilde{\Sigma}_t + g_t^\sigma \odot h_t^\sigma, \end{aligned} \quad (17)$$

where \odot is the Hadamard product. Here, g_t^μ, g_t^σ are the learned gating terms, which are passed through a sigmoid to ensure they are between zero and one. Meanwhile, h_t^μ, h_t^σ can be interpreted as the updates proposed by the network. In our experiments, this choice of parameterization significantly outperformed a simple fully-connected network.

B. Imitation Learning for Training the Optimizer

Unlike prior work in learning-to-optimize, we cannot assume that the optimization process itself is differentiable, as it occurs online via interactions with the environment. Even in the simulated case, we do not want to assume that everything has been implemented in a differentiable fashion. We could use reinforcement learning (RL), although it generally has high sample complexity and may be slow to learn. Since we have access to a tuned optimal controller, imitation learning is a promising direction for training the optimizer. Our expert is an MPPI controller with unrestricted access to samples. That is, we provide the controller with as many samples as needed to achieve good performance. The learner is also an MPPI controller, but it has access to fewer samples, and the standard update is replaced with the learned optimizer. In our preliminary experiments, we tried using standard behavioral cloning, in which we collect a dataset of expert demonstrations and train a policy offline via regression. However, this did

Algorithm 2: DAGGER Rollout Function

Input: State x_1 , policy $\pi_{\tilde{\theta}_1}$, probability β_k
Parameters: Rollout length T , expert samples N , learner samples M
Output: Shifted parameters $\tilde{\theta}_{1:T}$, sample costs $C_{1:T}^{(1:M)}$, expert decisions $\theta_{1:T}^{expert}$

for $t = 1, 2, \dots, T$ **do**
 Sample controls from policy $\{U_t^{(i)}\}_{i=1}^N \sim \pi_{\tilde{\theta}_t}$
 Sample $X_t^{(i)}$ from dynamics \hat{f} using $U_t^{(i)}, x_t$
 Compute costs $C_t^{(i)} \leftarrow C(X_t^{(i)}, U_t^{(i)})$
 Compute sample weights with Equation (9)
 Update $\tilde{\theta}_t$ to θ_t^{expert} using Equation (12)
 Sample $b \sim U(0, 1)$
 if $b \leq \beta_k$ **then**
 Set $\theta_t \leftarrow \theta_t^{expert}$
 else
 Update $\tilde{\theta}_t$ to θ_t^{learn} using Equation (17)
 Set $\theta_t \leftarrow \theta_t^{learn}$
 end
 Sample $u_t \sim \pi_{\theta_t}$ or use mean $u_t \leftarrow \mu_t$
 Apply control to system $x_{t+1} \sim f(x_t, u_t)$
 Shift parameters $\theta_{t+1} = \Phi(\theta_t)$
end

not work well due to covariate shift between the expert and learner distributions. Instead, we used DAGGER [56] to perform imitation learning, which is an interactive algorithm that aims to combat issues of covariate shift. The algorithm queries an expert online for corrective labels on learner visited states. We outline the main loop of DAGGER in Algorithm 1.

First, we begin by collecting a bootstrap dataset in which only the expert is run. Next, each iteration k of DAGGER, we run R rollouts according to Algorithm 2 by sampling some initial state x_1 from a known initial state distribution ρ . During a rollout, at each time step, we apply the controls from the expert with probability β_k and the learner with probability $1 - \beta_k$. The expert is always run in order to provide a corrective target for training the policy at the next iteration. Both the expert and learner controllers use the same trajectory samples, although the learner only receives a subset of them. Generally, the mixing probabilities β_k are set according to a schedule such that we run the learner more often in later iterations. In our experiments, we set $\beta_k = p^k$ for some $p \in (0, 1)$. After running the rollouts, we collect the warm-started control distribution parameters $\tilde{\theta}_{1:T}$, the trajectory costs $C_{1:T}^{(1:M)}$, and the updated expert control distribution parameters $\theta_{1:T}^{expert}$ into a dataset \mathcal{D}_i . We only collect the $M \leq N$ samples used by the learner. This data is then aggregated into our main dataset \mathcal{D} to train the optimizer.

IV. EXPERIMENTS

Implementation Details. In all experiments, our MPPI implementation is a modified version of the one developed by Bhardwaj et al. [6]. This implementation uses Halton sequences for generating control sequence samples and smooths the sampled trajectories with 3rd degree B-splines. We use a

fixed diagonal covariance for the sampling distribution and do not perform covariance adaptation. All hyperparameters were tuned using a grid search, and the optimal number of samples is what the expert controller has access to during data generation and training. Now, the optimal choice of hyperparameters may be different for a given number of samples. Therefore, for a fair comparison, we tune the MPPI hyperparameters separately for each sample count used in our evaluation. Both MPPI and the neural networks are implemented in PyTorch [57].

Task Details. We evaluate on simulated tasks:

- 1) **CARTPOLE:** The task is to slide a cart along a rail to swing up the pole attached via an unactuated joint using only actuation from the cart. Both the expert and learner are given access to the true analytical dynamics. The initial position of the cart and pole are randomized at every episode, which lasts 200 time steps. An episode is considered successful if the pole is swung up with a linear and angular velocity near zero.
- 2) **FRANKA REACHER:** A 7 degree-of-freedom (DOF) Franka Panda robot arm must reach a target goal from a fixed starting pose. The goal is randomly selected at the beginning of each episode. Both the expert and learner use the same kinematic model described in Bhardwaj et al. [6], which is different from the true dynamics of the simulator (Nvidia’s Isaac Gym [58]). Each episode lasts for 500 time steps and is considered successful if the end effector reaches the target position.
- 3) **FRANKA OBSTACLES:** This task is identical to FRANKA REACHER, except now there are two spherical obstacles placed in the environment which the arm must avoid. The obstacle and the goal positions are randomized at the beginning of each episode, which lasts for 600 time steps. An episode is considered successful if the end effector reaches the goal while avoiding collisions.

Evaluation. We evaluate the performance of the learned optimizer by varying the number of samples, up to the amount used by the expert. For each sample amount, we compare against a standard MPPI implementation with access to the same number of samples as the learned controller over 30 test rollouts. All test rollouts use a fixed set of start states, goals, and obstacle locations. This is achieved by setting the random seed value to a pre-defined test seed. Our primary metric for comparison is success rate, which is defined as the percentage of times the task goal was achieved out of all trials. In the FRANKA OBSTACLES task, the placement of obstacles is randomized according to a pre-specified distribution. Therefore, this task allows us to evaluate the generalization capability of the learned optimizer to new environments which are drawn from a similar distribution. Additionally, we report statistics of the end effector test trajectories. Specifically, we compute a relative trajectory length and average jerk as the ratio between the statistics for the learned optimizer and baseline MPPI controller. The trajectory length is averaged over all test runs, while the jerk is averaged over only successful test runs.

TABLE I: Success Rate Across All Tasks.

	# Samples	MPPI	L2O-MPC
CARTPOLE	8	100.0	100.0
	4	60.00	96.67
	2	10.00	90.00
FRANKA REACHER	64	100.0	100.0
	32	90.00	100.0
	16	63.33	100.0
	8	20.00	80.00
	4	10.00	63.33
	2	3.333	16.67
FRANKA OBSTACLES	512	80.00	80.00
	256	76.67	80.00
	128	73.33	76.67
	64	63.33	76.67
	32	33.33	66.67
	16	6.667	46.67

Training Details. Prior work in learning-to-optimize made use of recurrent architectures which can account for the history of the gradients and optimization process. While we could potentially benefit from such an architecture, we found that a simple multi-layer perceptron (MLP) was sufficient to learn powerful optimizers. As such, in all experiments, the learned optimizer is represented with a two-layer MLP using ReLU activation functions. We use 1024, 2048, and 4096 hidden units per layer for the CARTPOLE, FRANKA REACHER, and FRANKA OBSTACLES tasks, respectively. To prevent overfitting, all networks are regularized with dropout [59] using a dropout probability of 0.1. We use the ADAM optimizer [52] with a learning rate of 10^{-3} for CARTPOLE and FRANKA REACHER and 10^{-4} for FRANKA OBSTACLES. We normalize the total trajectory costs based on the mean and standard deviation of the training dataset. For all tasks, we bootstrapped the dataset with 1024 trajectories, in which only the expert’s action was applied to the system. We ran DAGGER for 20 iterations with 128 rollouts per iteration and a mixing probability schedule $\beta_k = 0.8^k$. For each iteration, we train the networks on the aggregated dataset for 1000 epochs with a batch size of 8. The best performing network evaluated on a held-out validation set is saved and used in the next iteration of DAGGER.

V. RESULTS

We report the success rate for all tasks in Table I and refer to standard MPPI by **MPPI** and MPC with the learned optimizer by **L2O-MPC**. Success rate is computed for each task based on the criteria discussed in Section IV. For FRANKA OBSTACLES, not every randomly generated scenario is feasible. Hence, there is an upper-bound of an 80% success rate for both **MPPI** and **L2O-MPC**. We can see that the performance of **MPPI** quickly drops off as the number of control sequence samples is reduced. For CARTPOLE, the performance of **L2O-MPC** remains fairly consistent even with a lower number of samples. While the performance drop is more pronounced in the Franka experiments, **L2O-**

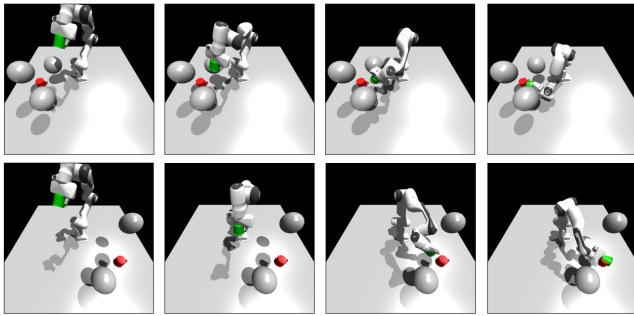


Fig. 1: Example trajectories of the FRANKA OBSTACLES task, in which the Franka arm end effector (green) is tasked with reaching the goal (red) while avoiding obstacles. The top row is a novel environment with three obstacles, while the bottom row is an environment from the test set.

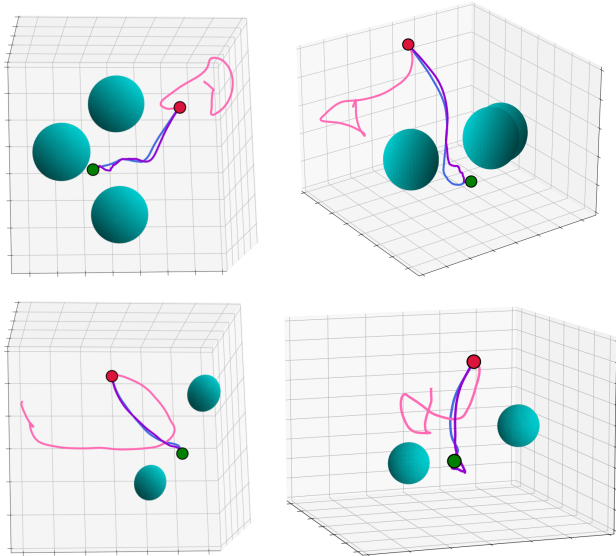


Fig. 2: Trajectories of the Franka arm end effector when controlled by **MPPI** with 512 samples (blue), **MPPI** with 16 samples (pink), and **L2O-MPC** with 16 samples (purple) to move from the starting position (red) to the goal (green) while avoiding obstacles (cyan). Plots in the same row are from the same environment but viewed from differing perspectives.

MPC still consistently matches or outperforms **MPPI** at each sample amount. In FRANKA REACHER, **L2O-MPC** is able to withstand a $4\times$ decrease in the number of samples while still achieving an 100% success rate. Similarly, in FRANKA OBSTACLES, **L2O-MPC** only incurs a 4% decrease in performance under an $8\times$ decrease in number of samples. This illustrates that **L2O-MPC** is successfully able to generalize to new environments similar to those on which it was trained.

Figure 1 illustrates two different example trajectories of the Franka arm avoiding different amounts of obstacles. These same environments are depicted in Figure 2, where we show end effector trajectories under **MPPI** with 512 samples, **MPPI** with 16 samples, and **L2O-MPC** with 16 samples. We can see that **MPPI** with 16 samples quickly diverges and is unable to reach the goal. On the other hand, **L2O-MPC** with 16 samples is able to better make use of the

TABLE II: Trajectory Statistics for FRANKA OBSTACLES.

# Samples	Length	Avg. Jerk
512	1.091	1.008
256	1.030	1.023
128	0.975	1.049
64	0.916	1.077
32	0.858	1.104
16	0.854	1.527

samples and still reach the goal while avoiding all obstacles. Moreover, the **L2O-MPC** controller was trained only on environments that contain two obstacles. Therefore, these results also indicate that the learned controller may generalize to novel environments on which it was not trained.

Qualitatively, the **L2O-MPC** trajectories appear to be slightly more jittery than the **MPPI** expert. In Table II, we provide the average relative jerk between **L2O-MPC** and **MPPI** for successful test runs at different sample counts. Indeed, we see that the **L2O-MPC** trajectories are less smooth than those of **MPPI**, and this effect is exacerbated at lower sample counts. Additionally, we provide the average relative trajectory length across all test environments. With more samples, **L2O-MPC** has slightly longer trajectories than **MPPI**, indicating that it is slower at reaching the goal. However, when given access to fewer samples, **L2O-MPC** consistently has shorter trajectories, as it more often reaches the goal. Therefore, while **L2O-MPC** is often jerkier and sometimes slower than the expert with full samples, it succeeds more often in achieving the desired objective in a timely fashion than **MPPI** given the same number of samples.

VI. CONCLUSION

We presented a method for improving upon standard sampling-based MPC algorithms by learning a better update rule. This provides a novel way to incorporate learning into model-based control algorithms, which is orthogonal to the standard approaches of learning or fine-tuning the dynamics model and/or cost function. We contend with noisy gradients by learning how to more effectively update the control distribution. By using structured sampling strategies, we are able to provide more information to the learned update and better utilize fewer samples. We show through empirical evaluations that our learned controllers remain competitive or outperform a baseline **MPPI** controller with access to the same number of samples. This demonstrates the viability of the learning-to-optimize framework in the context of control, opening the door for a variety of techniques to be applied to improving the performance of optimization-based controllers and planners. While we leveraged imitation learning to train the optimizers, this is just one possible option and an interesting direction for future work is to explore using reinforcement learning to see if it can outperform the expert and model-free methods. Since performance of sampling-based methods relies so heavily on thorough exploration of the sample space, another possible avenue is to learn how to generate better samples in addition to better updates.

REFERENCES

- [1] P. Abbeel, A. Coates, and A. Y. Ng, "Autonomous Helicopter Aerobatics through Apprenticeship Learning," *The International Journal of Robotics Research*, vol. 29, no. 13, pp. 1608–1639, 2010.
- [2] G. Williams, P. Drews, B. Goldfain, J. M. Rehg, and E. A. Theodorou, "Aggressive driving with model predictive path integral control," in *2016 IEEE International Conference on Robotics and Automation (ICRA)*. IEEE, 2016, pp. 1433–1440.
- [3] G. Williams, N. Wagener, B. Goldfain, P. Drews, J. M. Rehg, B. Boots, and E. A. Theodorou, "Information theoretic MPC for model-based reinforcement learning," in *2017 IEEE International Conference on Robotics and Automation (ICRA)*. IEEE, 2017, pp. 1714–1721.
- [4] N. Wagener, C.-A. Cheng, J. Sacks, and B. Boots, "An Online Learning Approach to Model Predictive Control," *arXiv preprint arXiv:1902.08967*, 2019.
- [5] V. Kumar, E. Todorov, and S. Levine, "Optimal Control with Learned Local Models: Application to Dexterous Manipulation," in *2016 IEEE International Conference on Robotics and Automation (ICRA)*. IEEE, 2016, pp. 378–383.
- [6] M. Bhardwaj, B. Sundaralingam, A. Mousavian, N. Ratliff, D. Fox, F. Ramos, and B. Boots, "STORM: An Integrated Framework for Fast Joint-Space Model-Predictive Control for Reactive Manipulation," *arXiv preprint arXiv:2104.13542*, 2021.
- [7] T. Erez, K. Lowrey, Y. Tassa, V. Kumar, S. Koley, and E. Todorov, "An integrated system for real-time Model Predictive Control of humanoid robots," in *2013 13th IEEE-RAS International Conference on Humanoid Robots (Humanoids)*. IEEE, 2013, pp. 292–299.
- [8] E. Hall and R. Willett, "Dynamical Models and Tracking Regret in Online Convex Programming," in *International Conference on Machine Learning (ICML)*. PMLR, 2013, pp. 579–587.
- [9] T. Chen, X. Chen, W. Chen, H. Heaton, J. Liu, Z. Wang, and W. Yin, "Learning to Optimize: A Primer and A Benchmark," *arXiv preprint arXiv:2103.12828*, 2021.
- [10] J. Kocijan, R. Murray-Smith, C. E. Rasmussen, and A. Girard, "Gaussian process model based predictive control," in *Proceedings of the 2004 American Control Conference (ACC)*, vol. 3. IEEE, 2004, pp. 2214–2219.
- [11] I. Lenz, R. A. Knepper, and A. Saxena, "DeepMPC: Learning Deep Latent Features for Model Predictive Control," in *Robotics: Science and Systems (RSS)*. Rome, Italy, 2015.
- [12] J. Fu, S. Levine, and P. Abbeel, "One-Shot Learning of Manipulation Skills with Online Dynamics Adaptation and Neural Network Priors," in *2016 IEEE/RSJ International Conference on Intelligent Robots and Systems (IROS)*. IEEE, 2016, pp. 4019–4026.
- [13] A. Nagabandi, G. Kahn, R. S. Fearing, and S. Levine, "Neural Network Dynamics for Model-Based Deep Reinforcement Learning with Model-Free Fine-Tuning," in *2018 IEEE International Conference on Robotics and Automation (ICRA)*. IEEE, 2018, pp. 7559–7566.
- [14] K. Chua, R. Calandra, R. McAllister, and S. Levine, "Deep Reinforcement Learning in a Handful of Trials using Probabilistic Dynamics Models," *arXiv preprint arXiv:1805.12114*, 2018.
- [15] D. Hafner, T. Lillicrap, I. Fischer, R. Villegas, D. Ha, H. Lee, and J. Davidson, "Learning Latent Dynamics for Planning from Pixels," in *International Conference on Machine Learning*. PMLR, 2019, pp. 2555–2565.
- [16] A. Tamar, G. Thomas, T. Zhang, S. Levine, and P. Abbeel, "Learning from the Hindsight Plan — Episodic MPC Improvement," in *2017 IEEE International Conference on Robotics and Automation (ICRA)*. IEEE, 2017, pp. 336–343.
- [17] M. Zhong, M. Johnson, Y. Tassa, T. Erez, and E. Todorov, "Value Function Approximation and Model Predictive Control," in *2013 IEEE Symposium on Adaptive Dynamic Programming and Reinforcement Learning (ADPRL)*. IEEE, 2013, pp. 100–107.
- [18] U. Rosolia and F. Borrelli, "Learning Model Predictive Control for iterative tasks. A Data-Driven Control Framework," *IEEE Transactions on Automatic Control*, vol. 63, no. 7, pp. 1883–1896, 2017.
- [19] K. Lowrey, A. Rajeswaran, S. Kakade, E. Todorov, and I. Mordatch, "Plan Online, Learn Offline: Efficient Learning and Exploration via Model-Based Control," *arXiv preprint arXiv:1811.01848*, 2018.
- [20] M. Bhardwaj, A. Handa, D. Fox, and B. Boots, "Information Theoretic Model Predictive Q-Learning," in *Learning for Dynamics and Control*. PMLR, 2020, pp. 840–850.
- [21] T. Wang and J. Ba, "Exploring Model-Based Planning with Policy Networks," *arXiv preprint arXiv:1906.08649*, 2019.
- [22] N. Wahlström, T. B. Schön, and M. P. Deisenroth, "From Pixels to Torques: Policy Learning with Deep Dynamical Models," *arXiv preprint arXiv:1502.02251*, 2015.
- [23] M. Watter, J. T. Springenberg, J. Boedecker, and M. Riedmiller, "Embed to Control: A Locally Linear Latent Dynamics Model for Control from Raw Images," *arXiv preprint arXiv:1506.07365*, 2015.
- [24] C. Finn and S. Levine, "Deep Visual Foresight for Planning Robot Motion," in *2017 IEEE International Conference on Robotics and Automation (ICRA)*. IEEE, 2017, pp. 2786–2793.
- [25] E. Banijamali, R. Shu, H. Bui, and A. Ghodsi, "Robust Locally-Linear Controllable Embedding," in *International Conference on Artificial Intelligence and Statistics*. PMLR, 2018, pp. 1751–1759.
- [26] F. Ebert, C. Finn, S. Dasari, A. Xie, A. Lee, and S. Levine, "Visual Foresight: Model-Based Deep Reinforcement Learning for Vision-Based Robotic Control," *arXiv preprint arXiv:1812.00568*, 2018.
- [27] J.-S. Ha, Y.-J. Park, H.-J. Chae, S.-S. Park, and H.-L. Choi, "Adaptive Path-Integral Autoencoder: Representation Learning and Planning for Dynamical Systems," *32nd Conference on Neural Information Processing Systems (NeurIPS)*, 2018.
- [28] A. Sharma, S. Gu, S. Levine, V. Kumar, and K. Hausman, "Dynamics-Aware Unsupervised Discovery of Skills," *arXiv preprint arXiv:1907.01657*, 2019.
- [29] B. Amos and D. Yarats, "The Differentiable Cross-Entropy Method," in *International Conference on Machine Learning (ICML)*. PMLR, 2020, pp. 291–302.
- [30] B. Amos, I. D. J. Rodriguez, J. Sacks, B. Boots, and J. Z. Kolter, "Differentiable MPC for End-to-end Planning and Control," *arXiv preprint arXiv:1810.13400*, 2018.
- [31] P. Karkus, D. Hsu, and W. S. Lee, "QMDP-Net: Deep Learning for Planning under Partial Observability," *arXiv preprint arXiv:1703.06692*, 2017.
- [32] M. Okada, L. Rigazio, and T. Aoshima, "Path Integral Networks: End-to-End Differentiable Optimal Control," *arXiv preprint arXiv:1706.09597*, 2017.
- [33] M. Okada and T. Taniguchi, "Acceleration of Gradient-based Path Integral Method for Efficient Optimal and Inverse Optimal Control," in *2018 IEEE International Conference on Robotics and Automation (ICRA)*. IEEE, 2018, pp. 3013–3020.
- [34] M. Pereira, D. D. Fan, G. N. An, and E. Theodorou, "MPC-Inspired Neural Network Policies for Sequential Decision Making," *arXiv preprint arXiv:1802.05803*, 2018.
- [35] A. Tamar, Y. Wu, G. Thomas, S. Levine, and P. Abbeel, "Value Iteration Networks," *arXiv preprint arXiv:1602.02867*, 2016.
- [36] A. Srinivas, A. Jabri, P. Abbeel, S. Levine, and C. Finn, "Universal Planning Networks: Learning Generalizable Representations for Visuomotor Control," in *International Conference on Machine Learning (ICML)*. PMLR, 2018, pp. 4732–4741.
- [37] T. Yu, G. Shevchuk, D. Sadigh, and C. Finn, "Unsupervised Visuomotor Control through Distributional Planning Networks," *arXiv preprint arXiv:1902.05542*, 2019.
- [38] M. Bhardwaj, B. Boots, and M. Mukadam, "Differentiable Gaussian Process Motion Planning," in *2020 IEEE International Conference on Robotics and Automation (ICRA)*. IEEE, 2020, pp. 10 598–10 604.
- [39] M. Andrychowicz, M. Denil, S. Gomez, M. W. Hoffman, D. Pfau, T. Schaul, B. Shillingford, and N. De Freitas, "Learning to learn by gradient descent by gradient descent," in *Advances in Neural Information Processing Systems (NeurIPS)*, 2016, pp. 3981–3989.
- [40] S. Ravi and H. Larochelle, "Optimization as a Model for Few-Shot Learning," *International Conference on Learning Representations (ICLR)*, 2016.
- [41] K. Lv, S. Jiang, and J. Li, "Learning Gradient Descent: Better Generalization and Longer Horizons," in *International Conference on Machine Learning (ICML)*. PMLR, 2017, pp. 2247–2255.
- [42] Y. Chen, M. W. Hoffman, S. G. Colmenarejo, M. Denil, T. P. Lillicrap, M. Botvinick, and N. Freitas, "Learning to Learn without Gradient Descent by Gradient Descent," in *International Conference on Machine Learning (ICML)*. PMLR, 2017, pp. 748–756.
- [43] T. Chen, W. Zhang, Z. Jingyang, S. Chang, S. Liu, L. Amini, and Z. Wang, "Training Stronger Baselines for Learning to Optimize," *Advances in Neural Information Processing Systems*, vol. 33, 2020.
- [44] K. Li and J. Malik, "Learning to Optimize," *arXiv preprint arXiv:1606.01885*, 2016.
- [45] J. X. Wang, Z. Kurth-Nelson, D. Tirumala, H. Soyer, J. Z. Leibo, R. Munos, C. Blundell, D. Kumaran, and M. Botvinick, "Learning to reinforcement learn," *arXiv preprint arXiv:1611.05763*, 2016.

- [46] K. Li and J. Malik, "Learning to Optimize Neural Nets," *arXiv preprint arXiv:1703.00441*, 2017.
- [47] I. Bello, B. Zoph, V. Vasudevan, and Q. V. Le, "Neural Optimizer Search with Reinforcement Learning," in *International Conference on Machine Learning (ICML)*. PMLR, 2017, pp. 459–468.
- [48] Y. Nesterov, "A method of solving a convex programming problem with convergence rate $\mathcal{O}(1/k^2)$," in *Sov. Math. Dokl.*, vol. 27.
- [49] N. Qian, "On the momentum term in gradient descent learning algorithms," *Neural Networks*, vol. 12, no. 1, pp. 145–151, 1999.
- [50] J. Duchi, E. Hazan, and Y. Singer, "Adaptive Subgradient Methods for Online Learning and Stochastic Optimization." *Journal of Machine Learning Research (JMLR)*, vol. 12, no. 7, 2011.
- [51] M. D. Zeiler, "ADADELTA: An Adaptive Learning Rate Method," *arXiv preprint arXiv:1212.5701*, 2012.
- [52] D. P. Kingma and J. Ba, "Adam: A Method for Stochastic Optimization," *arXiv preprint arXiv:1412.6980*, 2014.
- [53] S. J. Reddi, S. Kale, and S. Kumar, "On the Convergence of Adam and Beyond," *arXiv preprint arXiv:1904.09237*, 2019.
- [54] J. H. Halton, "Algorithm 247: Radical-inverse quasi-random point sequence," *Communications of the ACM*, vol. 7, no. 12, pp. 701–702, 1964.
- [55] K. Cho, B. Van Merriënboer, C. Gulcehre, D. Bahdanau, F. Bougares, H. Schwenk, and Y. Bengio, "Learning Phrase Representations using RNN Encoder-Decoder for Statistical Machine Translation," *arXiv preprint arXiv:1406.1078*, 2014.
- [56] S. Ross, G. Gordon, and D. Bagnell, "A Reduction of Imitation Learning and Structured Prediction to No-Regret Online Learning," in *Proceedings of the Fourteenth International Conference on Artificial Intelligence and Statistics (AISTATS)*. JMLR Workshop and Conference Proceedings, 2011, pp. 627–635.
- [57] A. Paszke, S. Gross, F. Massa, A. Lerer, J. Bradbury, G. Chanan, T. Killeen, Z. Lin, N. Gimelshein, L. Antiga, *et al.*, "Pytorch: An imperative style, high-performance deep learning library," *Advances in Neural Information Processing Systems (NeurIPS)*, vol. 32, pp. 8026–8037, 2019.
- [58] V. Makoviychuk, L. Wawrzyniak, Y. Guo, M. Lu, K. Storey, M. Macklin, D. Hoeller, N. Rudin, A. Allshire, A. Handa, *et al.*, "Isaac Gym: High Performance GPU-Based Physics Simulation For Robot Learning," *arXiv preprint arXiv:2108.10470*, 2021.
- [59] N. Srivastava, G. Hinton, A. Krizhevsky, I. Sutskever, and R. Salakhutdinov, "Dropout: A Simple Way to Prevent Neural Networks from Overfitting," *The Journal of Machine Learning Research (JMLR)*, vol. 15, no. 1, pp. 1929–1958, 2014.